

Alma Mater Studiorum Università di Bologna
Archivio istituzionale della ricerca

Blood metabolomics uncovers inflammation-associated mitochondrial dysfunction as a potential mechanism underlying ACLF

This is the final peer-reviewed author's accepted manuscript (postprint) of the following publication:

Published Version:

Moreau, R., Clària, J., Aguilar, F., Fenaille, F., Lozano, J., Junot, C., et al. (2020). Blood metabolomics uncovers inflammation-associated mitochondrial dysfunction as a potential mechanism underlying ACLF. JOURNAL OF HEPATOLOGY, 72(4), 688-701 [10.1016/j.jhep.2019.11.009].

Availability:

This version is available at: <https://hdl.handle.net/11585/709597> since: 2021-02-15

Published:

DOI: <http://doi.org/10.1016/j.jhep.2019.11.009>

Terms of use:

Some rights reserved. The terms and conditions for the reuse of this version of the manuscript are specified in the publishing policy. For all terms of use and more information see the publisher's website.

This item was downloaded from IRIS Università di Bologna (<https://cris.unibo.it/>).
When citing, please refer to the published version.

(Article begins on next page)

JHEPAT-D-19-01332-R2

Blood metabolomics uncovers inflammation-associated mitochondrial dysfunction as a potential mechanism underlying ACLF

Short title: Blood metabolome in ACLF

Richard Moreau^{1,2,*}, Joan Clària^{1,3,4,*}, Ferran Aguilar^{1,*}, François Fenaille^{5,*}, Juanjo Lozano⁴, Christophe Junot⁵, Benoit Colsch⁵, Paolo Caraceni⁶, Jonel Trebicka^{1,7}, Marco Pavesi¹, Carlo Alessandria⁸, Frederik Nevens⁹, Faouzi Saliba¹⁰, Tania M. Welzel⁷, Agustin Albillos¹¹, Thierry Gustot¹², Javier Fernández^{1,3,4}, Christophe Moreno¹², Maurizio Baldasarre⁶, Giacomo Zaccherini⁶, Salvatore Piano¹³, Sara Montagnese¹³, Victor Vargas¹⁴, Joan Genescà¹⁴, Elsa Solà^{3,4}, William Bernal¹⁵, Noémie Butin⁵, Thaïs Hautbergue⁵, Sophie Cholet⁵, Florence Castelli⁵, Christian Jansen¹⁶, Christian Steib¹⁷, Daniela Campion⁸, Raj Mookerjee¹⁸, Miguel Rodríguez-Gandía¹¹, German Soriano¹⁹, François Durand², Daniel Bente²⁰, Rafael Bañares²¹, Rudolf E Stauber²², Henning Gronbaek²³, Minneke J Coenraad²⁴, Pere Ginès^{3,4}, Alexander Gerbes¹⁷, Rajiv Jalan¹⁸, Mauro Bernardi⁶, Vicente Arroyo¹ and Paolo Angeli^{1,13} for the CANONIC Study Investigators of the EASL Clif Consortium, Grifols Chair and the European Foundation for the Study of Chronic Liver Failure (EF Clif).

¹EF Clif, EASL-CLIF Consortium and Grifols Chair, Barcelona, Spain; ²Inserm, U1149, Centre de Recherche sur l'Inflammation (CRI); UMRS1149, Université de Paris; Service d'Hépatologie, Hôpital Beaujon, Assistance Publique-Hôpitaux de Paris, Clichy; France; ³Hospital Clínic-IDIBAPS, Universitat de Barcelona, Barcelona, Spain; ⁴CIBERehd, Barcelona, Spain; ⁵Service de Pharmacologie et Immuno-Analyse (SPI),

Laboratoire d'Etude du Métabolisme des Médicaments, CEA, INRA, Université Paris Saclay, MetaboHUB, F-91191 Gif-sur-Yvette, France; ⁶Department of Medical and Surgical Sciences, University of Bologna, Bologna, Italy; ⁷J.W. Goethe University Hospital, Frankfurt, Germany; ⁸Division of Gastroenterology and Hepatology, San Giovanni Battista Hospital, Torino, Italy; ⁹University Hospital Gasthuisberg, KU Leuven, Belgium; ¹⁰Hôpital Paul Brousse, Université Paris-Sud, Villejuif, France; ¹¹Hospital Ramón y Cajal, Madrid, Spain; ¹²CUB Hôpital Erasme, Université Libre de Bruxelles, Brussels, Belgium; ¹³Unit of Internal Medicine and Hepatology, Dept. of Medicine, DIMED, University of Padova, Italy; ¹⁴Liver Unit, Hospital Universitari Vall d'Hebron, Vall d'Hebron Institute of Research (VHIR), Universitat Autònoma de Barcelona, Barcelona, Spain; ¹⁵Liver Intensive Therapy Unit, Institute of Liver Studies, Division of Inflammation Biology, King's College London, London, UK; ¹⁶Department of Internal Medicine I, University of Bonn, Germany; ¹⁷Department of Medicine II, Liver Center Munich, University Hospital LMU Munich, Munich, Germany; ¹⁸Liver Failure Group, Institute for Liver Disease Health, University College London, Royal Free Hospital, London, UK; ¹⁹Department of Gastroenterology, Hospital de la Santa Creu i Sant Pau, Universitat Autònoma de Barcelona, Barcelona, Spain; ²⁰University Hospital Hamburg-Eppendorf, Germany; ²¹Facultad de Medicina, Universidad Complutense, Madrid, Spain; ²²Medical University of Graz, Graz, Austria; ²³Department of Hepatology & Gastroenterology, Aarhus University Hospital, Aarhus, Denmark; ²⁴Department of Gastroenterology and Hepatology, Leiden University Medical Center, Leiden, The Netherlands;

*Share first authorship

An Appendix with the alphabetical list of CANONIC Study Investigators is provided.

Corresponding author: Richard Moreau, MD, INSERM U1149, Centre de Recherche sur l'Inflammation (CRI), 16 rue Henri Huchard, 75890 PARIS cedex 18, France. e-mail: richard.moreau@inserm.fr

Key words: Biomarkers; Multiorgan failure, Small-molecules; Lipidomics; CANONIC study.

Electronic word count: 5810

Number of Tables: 3

Number of Figures: 5

Conflicts of interest: Dr. Durand consults and received grants from Gilead and Astellas; he consults for Bristol-Myers Squibb. Dr. Ginès received Investigator sponsored research funding within the past two years from: Gilead, Mallinckrodt Pharmaceuticals, and Grifols. Dr. Ginès has participated in advisory board meetings for: Grifols, Gilead, Intercept, Martin Pharmaceuticals, Mallinckrodt Pharmaceuticals, Promethera and Sequana Medical (past 2 years). Dr. Jalan has research collaborations with Yaqrit and Takeda. Dr. Jalan is the inventor of OPA, which has been patented by UCL and licensed to Mallinckrodt Pharma. He is also the founder of Yaqrit limited, a spin out company from University College London and Thoeiris Ltd. The remaining authors disclose no conflicts.

Financial support: The study was supported by the European Foundation for the Study of Chronic Liver Failure (EF-Clif). The EF-Clif is a non-profit private organization. Jonel Trebicka is an EF-Clif Visiting Professor. Pere Ginès is a recipient of the ICREA ACADEMIA Award. The EF-Clif receives unrestricted donations from Cellex Foundation and Grifols, and is partner or contributor in several EU Horizon 2020 program projects. The funders had no influence on study design, data collection and analysis, decision to publish or preparation of the manuscript.

Author Contributions: Study concept and design (RM, JC, VA, PA); acquisition of metabolomics data (FF, NB, CJ, BC, SC); acquisition of clinical data and samples (PC, JT, CA, FN, FS, TMW, AA, TG, JF, CM, MB, GZ, SP, SM, VV, JG, ES, WB, CJ, CS, DC, RMoo, MRG, GS, FD, DB, RB, RES, HG, MJC, PG, AG, RJ, MB, PA); bioinformatics and statistical analysis (FA, JL, MP, NB, TH, FC); integration of clinical and biological results and interpretation of data (RM, JC, VA); drafting of the manuscript (RM, JC, VA); critical revision of the manuscript for important intellectual content (JT, PG, AG, RJ, MB); study supervision (RM, VA, PA).

Abstract

Background & aims: Acute-on-chronic liver failure (ACLF), which develops in patients with cirrhosis, is characterized by intense systemic inflammation and organ failure(s). Because systemic inflammation is energetically expensive, its metabolic costs may result in organ dysfunction/failure. Therefore, we aimed to analyze blood metabolome in patients with cirrhosis, with and without ACLF.

Methods: We performed untargeted metabolomics using liquid chromatography coupled to high-resolution mass spectrometry in serum from 650 patients with AD (acute decompensation of cirrhosis, without ACLF), 181 with ACLF, 43 with compensated cirrhosis, and 29 healthy subjects.

Results: Of the 137 annotated metabolites identified, 100 were increased in patients with ACLF of any grade, relative to those with AD, and 38 composed a distinctive blood metabolite fingerprint for ACLF. Among patients with ACLF, the intensity of the fingerprint increased across ACLF grades, and was similar in patients with kidney failure and in those without, indicating that the fingerprint reflected not only decreased kidney excretion but also altered cell metabolism. The higher the ACLF-associated fingerprint intensity, the higher plasma levels of inflammatory markers, tumor necrosis factor α , soluble CD206, and soluble CD163. ACLF was characterized by intense proteolysis and lipolysis; amino acid catabolism; extra-mitochondrial glucose metabolism through glycolysis, pentose phosphate, and D-glucuronate pathways; depressed mitochondrial ATP-producing fatty acid β -oxidation; and extra-mitochondrial amino acid metabolism giving rise to metabolites which are metabotoxins.

Conclusions: In ACLF, intense systemic inflammation is associated with blood metabolite accumulation witnessing profound alterations in major metabolic

pathways, in particular inhibition in mitochondrial energy production, which may contribute to the existence of organ failures.

Word count: 256

Lay summary

A 38-metabolite blood fingerprint specific for ACLF reveals a mitochondrial dysfunction in peripheral organs that may contribute to organ failures.

Introduction

The results of the CANONIC study were used to redefine acute-on-chronic liver failure (ACLF) as a syndrome which develops in patients with cirrhosis and acute decompensation (AD) and is characterized by an intense systemic inflammation^{1,2-4} associated with different combinations of organ failures among the six major organ systems (liver, kidney, brain, coagulation, circulation, and respiration), giving rise to different clinical phenotypes¹. ACLF is very frequent, affecting 30%-40% of hospitalized patients, and is associated with high short-term mortality rate (30% at 28 days)¹. In most cases of ACLF, the activation of innate immune cells by pathogen-associated molecular patterns (PAMPs) are thought to play a major role in the induction of systemic inflammation.⁵ However, the intrinsic mechanisms of ACLF at the tissue and cellular levels that contribute to the development and maintenance of organ failures are unknown. Understanding these mechanisms should not only result in progresses in the knowledge on pathophysiology of ACLF, but also could provide clues to the development of new biomarkers of organ dysfunction/failure and identification of targets for new therapies of organ failures which are urgently needed.

PAMP-elicited systemic inflammation stimulates the hypothalamic-pituitary adrenal axis to produce cortisol, glucagon, and adrenaline, which, in turn, induce rapid and widespread catabolism including glycogenolysis (liver), proteolysis (mainly muscles) and lipolysis (adipose tissue).⁶⁻⁸ This exuberant catabolic process results in the release of nutrients (glucose, amino acids and fatty acids [FAs], respectively) to fuel the energetically expensive immune responses (which include the production of a battery of inflammatory mediators, immune cell proliferation, adhesion and migration, respiratory burst, and production of acute-phase proteins).^{6,9} For example, during sepsis (which is a paradigm of acute systemic inflammation), glucose is

reallocated to activated innate immune cells where it is used to rapidly generate ATP through glycolysis, while mitochondrial oxidative phosphorylation (OxPhos) is suppressed^{6,7,9} (See glucose metabolism in naïve and activated innate immune cells, in Fig. S1A and S1B, respectively). Sepsis also induces metabolic changes in peripheral organs where it inhibits mitochondrial β -oxidation of FAs, resulting in decreased energy production and blood accumulation of FAs attached to molecules of carnitine^{8,10} (See FA metabolism under healthy conditions and during sepsis, in Fig. S2A and S2B, respectively). Therefore, in ACLF, systemic inflammation should lead to profound changes in most metabolic pathways.

Metabolomics, which identifies and quantifies small-molecule metabolites (the metabolome), is the omics closest to clinical phenotypes.¹¹ Interestingly, metabolites not only reflect the metabolic activity of tissues but, because many metabolites have powerful biological activity on critical pathophysiological processes, they can also influence the clinical phenotype.¹¹ The best approach to characterize the metabolic changes of such complex syndromes as ACLF, is to perform high throughput untargeted (agnostic) studies in large series of patients. This approach, which has been applied to sepsis,¹⁰ has so far not been applied in the investigation of ACLF.

Here, we report the results of an untargeted metabolomic investigation in biobanked sera from 831 patients with AD cirrhosis with and without ACLF, who were prospectively enrolled in the CANONIC study. The aims of the study were to characterize the metabolic profile associated with ACLF, to assess if there was a blood metabolite fingerprint specific for ACLF of any grade, each of the three ACLF grades of severity, and each of the three main organ failures (liver, brain, and kidney).

Patients and methods

Patients

The study used biobanked serum samples from patients with acutely decompensated cirrhosis (650 with AD (without ACLF); 181 with ACLF) prospectively enrolled in the CANONIC study¹, along with 43 patients with compensated cirrhosis, and 29 healthy subjects. All these individuals or their legal representatives and the ethics committee of each hospital involved in the study gave informed consent for omics investigations in the biobanked material. Values for physiological variables and markers of inflammation given in the manuscript were among those previously reported in other studies.^{1,2,4,12}

Definitions and diagnostic criteria of AD, organ failures (OFs) and organ dysfunctions (ODs), ACLF and its grades (-1, -2, and -3), are summarized in Table 1 and Fig. S3A.^{1,13}

Methods

Untargeted metabolomics by liquid chromatography coupled to high-resolution mass spectrometry (LC-HRMS)

Metabolic extracts were obtained from serum samples following methanol-assisted protein precipitation, and were then analyzed by liquid chromatography coupled to Exactive/Q-Exactive high-resolution mass spectrometers (Thermo Fisher Scientific, Courtaboeuf, France). A combination of two complementary chromatographic methods was used to profile metabolites.¹⁴ Data acquisition was performed in 5 independent batches while data normalization/standardization was achieved thanks to quality control samples injected at regular intervals. Data processing was achieved using the Workflow4Metabolomics platform.¹⁵ Annotation of metabolite features was

performed using an internal spectral database^{14,16} and corresponding chromatographic peak integration was conducted using the Trace Finder software (Thermo Fisher Scientific) (See Supplementary Methods).

Statistical analysis and data analysis

We performed multivariate models, including age and gender, and computed the area under the receiver-operating-characteristic curve (AUC) to estimate the value of each metabolite to discriminate patients with AD vs those with ACLF. Then, AUCs values were used for hierarchical cluster analysis (See Table 1 and Supplementary Methods).

Results

Patients With AD and ACLF exhibit different clinical phenotypes and features of systemic inflammation

Fig. S3B shows the remarkable heterogeneity of patients with ACLF, there being 35 different groups according to the number, types and combinations of OFs. Similarly, the 650 patients with AD without ACLF were highly heterogeneous, with only 288 of these presenting **AD without any organ failure/dysfunction** (data not shown). Fig. S3C shows the number of subjects with single-liver, -brain or -kidney failure/dysfunction (the 3 commonest affected organs in cirrhosis). Intense systemic inflammation was present in patients with AD and was even more marked in those with ACLF (Table 2).

ACLF associates with a set of increased blood metabolites

The different steps of the analysis of the metabolome are shown in Fig. S4. We identified and robustly monitored 137 annotated serum small-molecule metabolites (Table S1). Of note, some isomeric metabolites could not be resolved using the

presently used LC-HRMS approach. Thus, some chromatographic peaks could correspond to more than one metabolite (e.g., pentose phosphates) (Table S2).

PCA obtained from the entire cohort of study subjects (healthy subjects [HS], patients with compensated cirrhosis [CC], patients with AD and those with ACLF) showed clear distinction among the groups, with the first principal component accounting for 22.4% of the variance of the annotated metabolites (Fig. 1A). This indicates that the progression from CC to ACLF was a major contributor for the variation in the blood metabolome relative to being healthy.

To explore the relationship between the study groups and the underlying patterns of blood metabolite levels, we performed a supervised two-way, hierarchical cluster analysis (Fig. 1B). This figure brought two major observations. The first is that the concentration of most metabolites were higher in ACLF, and discriminated these patients from those with AD and CC. The second, and most important, is that there were no decreases in metabolite levels that would differentiate ACLF from the other groups. Together these results indicate that the variation in the blood metabolome associated with ACLF is primarily characterized by increases in the levels of blood metabolites.

This feature is also illustrated in Fig. 1C, in which fold changes for each metabolite were compared in a pairwise fashion between ACLF, AD and CC patients to HS (hereafter referred to as ACLF/HS, AD/HS, and CC/HS, respectively). There was an increase in the number of upregulated metabolites (i.e., whose blood levels increased; right upper quadrant), from CC to AD and ACLF. Moreover, the number of metabolites upregulated by more than 4-fold was higher in ACLF than in AD. In contrast, there were no differences in the number of downregulated metabolites across the three pairwise comparisons. Together, these findings confirm the

increases in several blood metabolite levels as a prominent change in the metabolome associated with ACLF.

Using the results obtained in the ACLF/HS comparison as a reference, we ranked metabolites from the highest fold change value to the lowest value and drew a Cleveland plot showing fold changes of each metabolite across the three pairwise comparisons (Fig. 1D, right; Fig. S5). Zooming on the 50 top metabolites (Fig. 1D, left), it appeared that, for each metabolite, the increase in ACLF was greater than the increase in the two other patients' groups. With few exceptions, the increase obtained in AD was intermediate between the increase in ACLF and that in CC. For example, the metabolite peak called "pentose phosphates" was increased by ~362-fold in ACLF/HS (which was the highest change in this comparison), ~64-fold in AD/HS, and 16-fold in CC/HS (Fig. 1D, left). Together these findings identify a set of blood metabolites whose blood levels dramatically increased in AD and culminated in ACLF. Fig. S6 gives the fold changes in the entire set of 137 annotated metabolites.

Blood metabolites compose a fingerprint for ACLF of any grade

We wondered whether any combination(s) of blood metabolites could reduce the dimension of the data set and serve as a fingerprint of ACLF of any grade. To address this question, for each of the 137 metabolites, we computed, an AUC assessing the discriminating accuracy of the metabolite in differentiating ACLF of any grade from AD (Table S3). The resulting AUCs and associated *P* values were used for a hierarchical cluster analysis, which identified two clusters (Fig. 2A; Fig. S6). The first cluster, was the largest, and included 99 metabolites poorly associated with ACLF; the second cluster included 38 metabolites with a highly significant association with ACLF (AUC for ACLF ranging from 0.73 to 0.87, and significant *p* values [Fig.

2A(i); Table S3]). Thirty-six of the 38 metabolites, were significantly increased in ACLF/HS (Table S4). Finally, we computed an eigenmetabolite (i.e., a value which is representative of the 38-metabolite cluster) and correlated the eigenmetabolite with the stage of progression of the disease, from healthy status to ACLF via CC and AD. The eigenmetabolite progressively increased across the different stages of the disease and reached a maximum in ACLF (Fig. 2B). Collectively, these findings indicate that the 38-metabolite cluster can be seen as a fingerprint of blood metabolites which characteristically accumulated in ACLF, differentiating this syndrome from AD.

The blood metabolite fingerprint of ACLF discriminates each ACLF grade from AD

We next investigated the correlation of blood metabolome and ACLF grades. For each of the 137 metabolites, and for each ACLF grade, we calculated an AUC to assess the discriminating accuracy of the metabolite in differentiating the ACLF grade (1, 2 or 3) from AD (Table S3). Then, we created a three-column heatmap according to **increasing** severity [Fig. 2A(ii)] in which each row (one per metabolite) was sorted according to the hierarchical clustering of AUC for ACLF of any grade [Fig. 2A(i)]. Regarding the 38-metabolite cluster defining the ACLF fingerprint, the high AUC values observed in ACLF of any grade were maintained when patients were distributed across the ACLF grades (-1, -2, and -3) [Fig. 2A(ii)], indicating **similarities** of metabolome changes across ACLF grades. Of note, the blood metabolite fingerprint was already present in ACLF-1 indicating that this group is clearly different from the AD group, therefore giving biological basis to the clinical diagnostic criteria proposed by the CANONIC study. Another important finding was that the AUCs for

ACLF-1 or ACLF-2 had very close values which were lower than the corresponding AUC for ACLF-3. Consistent with these findings, the eigenmetabolite of the 38-metabolite cluster increased from AD to ACLF-1, plateaued between ACLF-1 and -2, and further increased in ACLF-3 (Fig. 2C).

A complete ACLF-associated blood metabolite fingerprint is seen in the absence of kidney failure/dysfunction

The presence of kidney failure or dysfunction is important to define ACLF.¹ The deterioration of kidney function can result in blood metabolite accumulation, due to both reductions in renal metabolite excretion and increases in metabolite production by the kidney.⁸ In our study, as expected,¹ the prevalence of kidney failure or dysfunction was high among patients with ACLF (Fig. S1B, S3C). Because of this high prevalence, the blood metabolite fingerprint identified in the whole group of patients with ACLF may, in fact, reflect changes in metabolome related to deteriorated kidney function. To address this question, we compared the eigenmetabolite of the 38-metabolite cluster across 3 groups: 318 patients with **AD without any organ failure/dysfunction**, 105 patients with single kidney failure/dysfunction and 68 patients with ACLF-2 or -3, without kidney failure/dysfunction. The eigenmetabolite was significantly higher in the single kidney-failure/dysfunction group than in the group **with AD without any organ failure/dysfunction** (Fig. 2D), confirming that deterioration in kidney function is associated with an intense blood metabolite fingerprint. However, the eigenmetabolite was similar in the “nonrenal”-ACLF group and the single kidney-failure/dysfunction group. Therefore, alterations in cell metabolism in nonrenal organs may contribute to the fingerprint associated with ACLF.

The blood metabolite fingerprint is qualitatively similar in patients with single organ dysfunction/failure independently of the affected organ

To assess if there was a specific blood metabolite fingerprint for each category of organ failure (OF)/organ dysfunction (OD), we compared patients with single liver-, brain- and kidney-failure/dysfunction with patients with **AD without any organ failure/dysfunction**, using metabolite AUCs [Fig. 2A(iii)]. The clinical phenotype and number of patients included in this analysis is depicted in Fig. S3C. The main finding of this analysis was that the fingerprint defining ACLF of any grade was also identified in the three categories of single OF/OD, suggesting a common metabolic derangement across different organs.

The blood metabolite fingerprint is similar in infection-related and infection-unrelated ACLF

In the general population, sepsis is known to alter blood metabolome.¹⁴ We wondered if among patients with ACLF, blood metabolome differed between those with bacterial infection (n=62) and those without infection (n=117). Using metabolite AUCs for ACLF versus AD, we found that the blood metabolite fingerprint was remarkably similar in the two groups of patients (Fig. 3), suggesting **similarities** in metabolic alterations underlying ACLF, whichever infection was present or not. **Of note, a group of 31 metabolites, which were not members of the fingerprint, had higher AUCs for sepsis-related ACLF than for sepsis-unrelated ACLF (Fig. 3).**

The blood metabolite fingerprint correlates with systemic inflammation

As expected,²⁻⁴ the plasma levels of many inflammatory mediators and biomarkers were increased in our patients with ACLF relative to AD (Table 1). On the other hand, acute systemic inflammation plays a major role in multiorgan metabolic reprogramming.^{6,8} Here, we found that the eigenmetabolite of the 38-metabolite cluster was positively and significantly correlated with several markers of inflammation, in particular soluble CD206, soluble CD163, and tumor necrosis factor α (TNF- α) (Fig. S7), suggesting that the intensity of systemic inflammation was associated with the “intensity” of the ACLF-associated metabolic alterations witnessed in the blood metabolite fingerprint.

Members of the ACLF blood metabolite fingerprint have potential pathophysiological significance

ACLF associates with increased proteolysis and lipolysis

As expected in the context of acute systemic inflammation,^{6,8} several members of the ACLF-associated 38-metabolite cluster were amino acids or amino acid metabolites indicating increased proteolysis (e.g., saccharopine, an intermediate in the degradation of lysine, and N6,N6,N6-trimethyl-L-lysine, a product of protein-bound lysine degradation) (Fig. 2A) (Supplementary results).

ACLF associates with changes in intracellular glucose metabolism

Consistent with previous findings in acute systemic inflammation,⁹ ACLF was associated with features of increased activity of the pentose phosphate pathway (Fig. 2A; Fig. 4). The 38-metabolite cluster also included metabolites indicating increase in the glucuronate pathway (Fig. 2A; Fig. 4). ACLF also exhibited increased blood levels of the glucose metabolite lactic acid (Fig. S8). Finally, the 38-metabolite cluster included 4-hydroxy-3-methoxyphenylglycol sulfate (Fig. 2A), indicating increased

sympathetic nervous activity, a stimulus for glycolysis. Together, these data indicate that ACLF was associated with intracellular glucose rerouting through different extramitochondrial pathways (Fig. 4; Table S5).

ACLF is associated with reduced mitochondrial β -oxidation

Fatty acylcarnitines (i.e., FAs attached to carnitine) of different lengths (two being in the 38-metabolite cluster [Fig. 2A]) had increased blood levels in ACLF/HS comparison (Fig. 5A). Blood accumulation of fatty acylcarnitines is a marker of decreased mitochondrial β -oxidation and subsequent reduction in OxPhos (Fig. 5B),^{8,10} in particular in the context of acute systemic inflammation.^{8,10} Of note, N6,N6,N6-trimethyl-L-lysine, which is a known precursor of carnitine (Fig. 5B) was also a member of the 38-metabolite cluster. Interestingly, an associated lipidomic analysis of a partly overlapping patient cohort has been conducted (data not yet published) suggesting that ACLF may lead to increased levels of the monounsaturated FAs palmitoleic and oleic acids, which in the context of ACLF reflects both lipolysis in adipose tissue and decrease oxidation in peripheral tissues.⁸

Accentuation of metabolism alterations in sepsis-related ACLF

The analysis of the group of 31 fingerprint-independent metabolites that have higher AUC for sepsis-related ACLF than for ACLF unrelated to sepsis (Fig. 3) revealed that several of these metabolites were related to glycolysis (pyruvate, lactic acid), extraction of intermediates of the Krebs' cycle (citric acid/isocitric acid, oxaloacetic acid), and fatty acylcarnitines (butyrylcarnitine, decanoylcarnitine). Together these findings suggest that sepsis-related ACLF was associated with more intense glycolysis (see Fig. S1) and more marked inhibition of β -oxidation.

Discussion

This article reports the first study using high-throughput untargeted metabolomics in blood samples from a large series of patients with AD of cirrhosis, with or without ACLF, patients with compensated cirrhosis and healthy subjects. We found that ACLF occurs in the setting of marked and widespread alterations in cellular metabolism leading up to a specific metabolome profile (fingerprint) made of 38 blood metabolites which have increased levels in ACLF. Of note, the ACLF fingerprint was independent of the type of organ failure (phenotype). We found a direct correlation between the plasma levels of markers for systemic inflammation (a hallmark of ACLF)¹⁻⁴ and the eigenmetabolite (which is representative of the fingerprint), suggesting a close link between systemic inflammation and the alterations in cell metabolism captured by the blood metabolite fingerprint.

Our study also showed that, among patients with ACLF, the blood metabolite fingerprint was similar among those who had bacterial infection (i.e., sepsis) at enrollment and those who did not have this complication. ACLF mainly occurs in two apparently different contexts; in the first one, ACLF develops in the context of bacterial sepsis (even if the cause of hospital admission was severe alcoholic hepatitis or gastrointestinal hemorrhage), while in the second one, ACLF develops without a clinically identifiable trigger (infection, trauma, burns, pancreatitis, or hypovolemic shock),^{1,5,17-19} a condition we called ACLF of unknown origin. It has been proposed that the inducers of systemic inflammation in sepsis-related ACLF are bacterial molecules (the paradigm of these being PAMPs) produced by infecting bacteria, while, in ACLF of unknown origin, the inducers of systemic inflammation are PAMPs which have translocated from the gut to the systemic circulation, and are unrelated to any ongoing infection.^{5,17,19} Both forms of ACLF (sepsis-related versus

unknown origin), therefore, would have mechanistic similarities, i.e., primarily an exaggerated response of the innate immune system to bacterial PAMPs. Shared mechanisms would explain an identical 38-metabolite blood fingerprint in patients with sepsis-related ACLF and in those with ACLF of unknown origin. The fact that the systemic inflammatory response is more intense among patients with sepsis-related ACLF than among those with ACLF of unknown origin,² may explain that some alterations in fingerprint-independent metabolites were more marked in the former patients than in the latter (Fig.3).

PAMP-induced acute systemic inflammation is known to stimulate the hypothalamic-pituitary-adrenal axis and sympathetic nervous system to activate glycogenolysis, proteolysis and lipolysis.⁶⁻⁸ Intense catabolism also occurred in ACLF, reflected here by blood accumulation of FAs and 24 metabolites derived from amino acids. In addition our patients with ACLF had features of extreme activation of the sympathetic nervous activity, indicated by the accumulation of the catecholamine metabolite 4-hydroxy 3-methoxyphenylglycol sulfate. The purpose of this coordinated neurohumoral response is to provide nutrients to the energetically expensive inflammatory responses; the overall cost having been estimated to reach up 10,000 calories/day for a septic patient.⁷

In our patients with ACLF, glucose metabolism occurred primarily in the cytosol, and not in the mitochondria. Indeed, we found evidence of enhanced glycolysis because of accumulation of pentose phosphates (fingerprint; Fig. 4) and lactic acid (Fig. S8). Moreover, the fingerprint included glucuronic acid, another cytosolic metabolite of glucose, which can give rise to pentose phosphates (Fig. 4). This rerouting in the intracellular glucose metabolism also occurs in other stress conditions.⁶⁻¹⁰ In the context of PAMP-induced systemic inflammation, glucose is

prioritized to activated innate immune cells to rapidly produce ATP through an activation of glycolysis (caused by the induction of the key enzymes of this pathway) giving rise to lactate, while, at the same time mitochondrial OxPhos is suppressed (for several reasons, including the inhibition of the electron transport chain by overproduced nitric oxide [NO])^{6,7,9} (Fig. S1B). In activated innate immune cells, glucose also enters the pentose phosphate pathway, a branch of glycolysis which provides riboses (essential for the synthesis of nucleotides to support production of inflammatory molecules) and NADPH (a crucial cofactor of lipid synthesis and for NADPH oxidase activity which produces microbicidal reactive oxygen species [ROS])⁹ (Fig. S1B). Therefore, in PAMP-induced systemic inflammation, glucose is reallocated to innate immune cells to support the vigorous anabolic, defense response produced by these cells. Together these findings suggest that the ACLF metabolite fingerprint primarily captured changes in glucose metabolism that occurred in activated innate immune cells, although the contribution of other tissues cannot be excluded.

An important finding of our study was the blood accumulation, in ACLF, of fatty acylcarnitines (fingerprint; Fig. 5A). In peripheral (non-immune) organs, in the context of PAMP-induced systemic inflammation, there is a reduction of FA catabolism through mitochondrial β -oxidation.^{7,8} Systemic inflammation downregulates in these organs, the peroxisome proliferator-activated receptor (PPAR)- α target-genes involved in mitochondrial β -oxidation and downregulates the enzyme responsible for translocating fatty acylcarnitines into the mitochondrial matrix⁸ (Fig. S2B). Blood accumulation of fatty acylcarnitines witnesses the systemic inflammation-induced inhibition of β -oxidation.^{7,8,10} Therefore, our finding of increased blood levels of fatty acylcarnitines in patients with ACLF indicates that these patients have marked

reduction in mitochondrial β -oxidation in **peripheral organs** (Fig. 5B). The Krebs' cycle produces much more ATP through complete oxidation of FAs (Fig. S2A) than through glucose oxidation (Fig. S1A). Therefore, in ACLF, the suppression of mitochondrial β -oxidation likely results in a dramatic decrease in FA-derived energy supply in peripheral organs. Moreover, like in sepsis,⁷ the accumulation of “non-oxidized” FAs and the stimulation of mitochondrial ROS production by inflammation may also occur in ACLF and cause mitochondrial damage. Together, these findings strongly suggest that, in ACLF, a marked mitochondrial dysfunction occurs in peripheral organs, contributing to the development of organ failures.

Most steps of the amino acid metabolism occur outside the mitochondria and this may explain why they are not highly affected by mitochondrial dysfunction. Accordingly, there was increased generation and accumulation of many blood amino acid metabolites associated with ACLF, which is not only related to the increased proteolytic release of amino acids secondary to systemic inflammation and the acute stress response, but also to the activating effect of PAMPs and/or cytokines on several enzymatic reactions involved in amino acid metabolism. These reactions give rise to derivatives with substantial biological effects including inflammation, immunomodulation, generation of ROS, NO, CO, and H₂S, vasodilation, neurotoxicity and endothelial dysfunction, among others (Table 2; **Supplementary Results section**). These changes may contribute to the pathophysiology of many complications associated with ACLF.

Together, these observations suggest that sepsis and ACLF share pathophysiological mechanisms leading to organ failures; cytokine-induced changes in stress hormone response and in the generation of ROS, NO, CO, and H₂S would be the initial effectors, impairment in mitochondrial activity and metabolic suppression

the intermediate step, and organ failure the final consequence. The mitochondrial dysfunction and subsequent metabolic and energetic cellular crisis associated with severe systemic inflammation have been traditionally attributed to damage of the mitochondrial membranes due to oxidative stress, which is the site where ATP is generated. However, there are preliminary evidences that transient mitochondrial dysfunction and metabolic suppression could also represent an adaptive and functional response like hibernation, that prevents a dramatic decrease of ATP below levels compatible with life and progression of cell dysfunction to cell death.⁸ Decline in organ function(s) would therefore be the cost paid to cope with organismal energetic demand. This hypothesis, which is being intensively investigated by the basic, translational and clinical investigators in the fields of infectious diseases, intensive care and nephrology from past decades, has never been proposed for cirrhosis. Our metabolomic data strongly support this hypothesis.

The fact that our study was associative and did not include mechanistic investigations should be taken into account and our results be interpreted with caution. There are multiple objectives for future research on ACLF, and some examples are discussed now. Future research, using animal models of ACLF, should use high-throughput metabolomics and transcriptomics to investigate the metabolic state in each of the major target organs, i.e., the liver, kidney, brain, heart, and skeletal muscles. The interest of such integrated approaches is highlighted by a recent study which revealed the existence of hepatic reprogramming of FA oxidation (i.e., major downregulation of PPAR- α target genes) in non-cirrhotic mice challenged with the PAMP lipopolysaccharide.⁸ Future research should also elucidate the molecular mechanisms by which systemic inflammation results in downregulation of PPAR- α target genes. This will identify targets for novel therapeutic approaches that

would be able to upregulate PPAR- α -target genes and therefore stimulate β -oxidation of FA and restore energy production in peripheral organs. Future research should also address the question of whether the use of some blood metabolite levels on the top of currently used prognostic markers would refine the prediction of outcome among patients with acutely decompensated cirrhosis, with and without ACLF. Of note, in the context of severe sepsis in the general population, higher blood levels of fatty acylcarnitines have been found to be associated with a higher risk of death.¹⁰

In conclusion, in ACLF, intense systemic inflammation is associated with blood metabolite accumulation indicating marked alterations in major metabolic pathways, in particular mitochondrial dysfunction which may be involved in the existence of organ failures. This study can serve as a resource for future studies of metabolism alterations in decompensated cirrhosis.

Acknowledgements: We thank the IDIBAPS Biobank for careful assistance in the handling of samples.

References

1. Moreau R, Jalan R, Gines P, et al. Acute-on-chronic liver failure is a distinct syndrome that develops in patients with acute decompensation of cirrhosis. *Gastroenterology* 2013;144:1426-1437, 1437.
2. **Clària J, Stauber RE**, Coenraad MJ, et al. Systemic inflammation in decompensated cirrhosis. Characterization and role in acute-on-chronic liver failure. *Hepatology* 2016;64:1249-1264.
3. Solé C, Solà E, Morales-Ruiz M, et al. Characterization of Inflammatory Response in Acute-on-Chronic Liver Failure and Relationship with Prognosis. *Sci Rep* 2016;6:32341.
4. Trebicka J, Amoros A, Pitarch C, et al. Addressing Profiles of Systemic Inflammation Across the Different Clinical Phenotypes of Acutely Decompensated Cirrhosis. *Front Immunol* 2019;10:476.
5. **Arroyo V, Moreau R, Kamath PS, et al. Acute-on-chronic liver failure in cirrhosis. *Nat Rev Dis Primers* 2016;2:16041.**
6. Wang A, Luan HH, Medzhitov R. An evolutionary perspective on immunometabolism. *Science* 2019;363:eaar3932.
7. Van Wyngene L, Vandewalle J, Libert C. Reprogramming of basic metabolic pathways in microbial sepsis: therapeutic targets at last? *EMBO Mol Med* 2018;10. pii: e8712.
8. Ganeshan K, Nikkanen J, Man K, et al. Energetic Trade-Offs and Hypometabolic States Promote Disease Tolerance. *Cell* 2019;177:399-413.
9. O'Neill LA, Pearce EJ. Immunometabolism governs dendritic cell and macrophage function. *J Exp Med* 2016;213:15-23.

10. Langley RJ, Tsalik EL, van Velkinburgh JC, et al. An integrated clinico-metabolomic model improves prediction of death in sepsis. *Sci Transl Med* 2013;5:195.
11. Guijas C, Montenegro-Burke JR, Warth B, et al. Metabolomics activity screening for identifying metabolites that modulate phenotype. *Nat Biotechnol* 2018;36:316-320.
12. **Clària J, Moreau R**, Fenaille F, et al. Orchestration of Tryptophan-Kynurenine pathway, acute decompensation and acute-on-chronic liver failure in cirrhosis. *Hepatology* 2019:1686-1701.
13. Jalan R, Saliba F, Pavesi M, et al. Development and validation of a prognostic score to predict mortality in patients with acute-on-chronic liver failure. *J Hepatol* 2014;61:1038-1047.
14. Boudah S, Olivier MF, Aros-Calt S, et al. Annotation of the human serum metabolome by coupling three liquid chromatography methods to high-resolution mass spectrometry. *J Chromatogr B Analyt Technol Biomed Life Sci* 2014;966:34-47.
15. Giacomoni F, Le Corguillé G, Monsoor M, et al. Workflow4Metabolomics: a collaborative research infrastructure for computational metabolomics. *Bioinformatics* 2015;31:1493-1495.
16. Roux A, Xu Y, Heilier JF, Olivier MF, et al. Annotation of the human adult urinary metabolome and metabolite identification using ultra high performance liquid chromatography coupled to a linear quadrupole ion trap-Orbitrap mass spectrometer. *Anal Chem* 2012;84:6429-6437.

17. **Fernández J, Clària J, Amorós A, et al.** Effects of Albumin Treatment on Systemic and Portal Hemodynamics and Systemic Inflammation in Patients With Decompensated Cirrhosis. *Gastroenterology* 2019;157:149-162
18. Sersté T, Cornillie A, Njimi H, et al. The prognostic value of acute-on-chronic liver failure during the course of severe alcoholic hepatitis. *J Hepatol* 2018;69:318-324.
19. Bernardi M, Moreau R, Angeli P, et al. Mechanisms of decompensation and organ failure in cirrhosis: From peripheral arterial vasodilation to systemic inflammation hypothesis. *J Hepatol* 2015;63:1272-1284.
20. Scott Chialvo CH, Che R, Reif D, et al. Eigenvector metabolite analysis reveals dietary effects on the association among metabolite correlation patterns, gene expression, and phenotypes. *Metabolomics* 2016;12:p1167.

Figure legends

Figure 1. Acute-on-chronic liver failure (ACLF) associates with a set of increased blood metabolites. (A) Principal components analysis of the metabolites across the four study groups. Contributions of persons (points) to the first two principal components (PC1 and PC2). (B) Supervised clustering analysis according to study groups. (C) Volcano plots showing the results of pairwise comparisons of blood metabolites levels in each patients' group relative to healthy subjects. The vertical dashed lines indicate the threshold for the two-fold abundance difference. The horizontal dashed line indicates the $p = 0.05$ threshold. (D) Cleveland plots. Right. The whole set of metabolites are ranked according to their fold changes in ACLF vs HS (the highest fold changes on the top; the lowest on the bottom). Fold changes in AD vs HS, and CC vs HS are also shown. Left inset, zooming on the 50 top metabolites in the three comparisons. Unless specified, the set of 137 identified annotated metabolites were used for analysis.

Figure 2. Identification of a unique ACLF-associated blood metabolite fingerprint and its behavior in different patients' groups. (A) (i) Hierarchical cluster analysis of the area under the receiver-operating-characteristic curve (AUCs) assessing the discriminating accuracy of each of the 137 metabolites in differentiating ACLF from AD; (ii) Corresponding metabolite AUC values in assessing ACLF-1, -2, and -3, relative to AD; (iii) Corresponding metabolite AUC values in assessing single failure/dysfunction of either the liver, brain or kidney liver, relative to **AD without any organ failure/dysfunction**. Vertical violet bar identify the 38-metabolite cluster highly associated with ACLF of any grade and composing the ACLF-associated blood metabolite fingerprint. (B) The eigenmetabolite²⁰ of the 38-metabolite cluster across

different groups, including healthy subjects, patients with compensated cirrhosis, patients with AD of cirrhosis (without ACLF) and patients with ACLF. (C) The eigenmetabolite of the 38-metabolite cluster across four groups: AD, ACLF-1, ACLF-2, ACLF-3. (D) The eigenmetabolite of the 38-metabolite cluster across three groups: **AD without any organ failure/dysfunction**, single kidney failure/dysfunction, ACLF-2 or -3 without kidney failure/dysfunction. ACLF denotes acute-on-chronic liver failure, AD acute decompensation, OD organ dysfunction, OF organ failure, HS healthy subjects, KF kidney failure, and KD kidney dysfunction.

Figure 3. Similarities of the blood metabolite fingerprint between patients with ACLF related to bacterial infection and those with ACLF unrelated to bacterial infection. See legend of Fig. 2 for methods. The vertical violet line indicates the 38 metabolites of the ACLF fingerprint. The vertical yellow line indicates the 31 metabolites associated with sepsis-related ACLF.

Figure 4. Channeling of intracellular glucose metabolism in ACLF. Under normal conditions, glucose is converted into glucose-6-phosphate which is initially metabolized in the cytosol by glycolysis, yielding pyruvate (glycolysis produces 2 molecules of pyruvate, 2 molecules of ATP and one molecule of the reduced form of nicotinamide adenine dinucleotide (NAD⁺) per mol of glucose [not shown]). At enough tissue O₂ tension, pyruvate is imported into the mitochondria and converted into acetyl-Coenzyme A (CoA). Acetyl-CoA then enters the Krebs' cycle leading to generation of CO₂ and the reduction of NAD⁺ and flavin adenine nucleotide (FAD). The reduced forms of NAD⁺ and FAD donate electrons to the electron transport chain (ETC) which uses O₂ as terminal electron acceptor. The whole process consumes O₂

and releases CO₂ (mitochondrial respiration). During the electron transfer process, protons are pumped from the mitochondrial matrix into the intermembrane mitochondrial space, resulting in an electrical potential across the inner mitochondrial membrane that provides the energy for ATP synthesis by complex V (ATP synthase). The process called oxidative phosphorylation (OxPhos) produces 17 ATP molecules from each pyruvate molecule (34 from each glucose molecule entering the glycolytic process) (not shown). Under certain conditions (e.g., acute systemic inflammation), glucose-6-phosphate enters the pentose phosphate pathway whose irreversible oxidative phase yields to the conversion of glucose-6-phosphate into D-ribulose 5-phosphate and generation of the reduced form of nicotinamide adenine dinucleotide phosphate (NADPH). The second phase of the pentose phosphate pathway is non-oxidative and reversible, and converts D-ribulose 5-phosphate into D-xylulose 5-phosphate or D-ribose 5-phosphate. D-ribose 5-phosphate can give rise to D-ribose 1-phosphate, connecting the pentose phosphate pathway to nucleotide synthesis. Finally, glucose-6-phosphate channeling in the glucuronate pathway can produce, via D-glucuronic acid, L-xylulose which, in turn, yields any of the metabolites referred to as “pentose alcohols”. L-xylulose, via xylitol, produces D-xylose whose end-product is D-threitol. D-xylulose, which is produced from xylitol, directly or via D-xylose, can yield D-xylulose 5-phosphate. In ACLF, glucose-6-phosphate can engage three pathways. The first one is glycolysis which can result in lactate production (because pyruvate does not enter the Krebs’ cycle). The other two pathways are the pentose phosphate and the glucuronate pathways. Highlighted are metabolites whose blood levels were increased in the ACLF group relative to healthy subjects. Some important enzymes are shown using their gene symbols; official full names are given in Table S5.

Figure 5. Fatty acylcarnitines accumulation in ACLF. (A) Names and characteristics of fatty acylcarnitines whose blood levels were increased in the ACLF group relative to healthy subjects. (B) Under normal conditions, free fatty acids (FFAs) are transported across the cell membrane by specific transporters and, once in the cytosol, they are coupled to Coenzyme A (CoA) by acyl-CoA synthase and shuttled across the inner mitochondrial membrane by the action of carnitine acyltransferases which release acyl-CoA into the mitochondrial matrix. Subsequently acyl-CoA is catabolized by β -oxidation under the action of acyl-CoA dehydrogenases. The process is conducted by cleaving two carbon molecules in every oxidation cycle to form acetyl-CoA. The cycle is repeated until the complete FA has been reduced to acetyl-CoA, which through oxidative phosphorylation (OxPhos) releases energy in the form of ATP. For example, the net β -oxidation energetic balance of a molecule of palmitate is the production of 129 molecules of ATP. Highlighted are the metabolites whose blood levels were increased in the ACLF group relative to healthy subjects.

Table 1. Glossary**Definitions for clinical data**

Acute decompensation (AD) of cirrhosis: Acute development of ascites, hepatic encephalopathy, gastrointestinal hemorrhage, or bacterial infection (in patients with prior AD), or any combination of these.¹

Organ failures and organ dysfunctions: Defined according to the Chronic Liver Failure-Consortium Organ Failure (OF) Scoring system.¹⁴ (See Figure S3A)

Acute-on-chronic liver failure (ACLF) grade-1 (or ACLF-1): Presence of single kidney failure or of any other type of single organ failure, if associated with brain or kidney dysfunction

ACLF grade-2 (ACLF-2): Presence of 2 organ failures

ACLF grade-3 (ACLF-3) : Presence of 3 to 6 organ failures

Absence of ACLF

(a) patients with acute decompensation of cirrhosis without any organ failure or organ dysfunction

(b) patients with single or multiple organ dysfunctions

(c) patients with single non-kidney organ failure without kidney or brain dysfunction.

Definitions for metabolome analyses (see also Supplementary Methods)

Principal components analysis (PCA): A technique used to reduce the dimension of data, eliminating those elements which are closely correlated.

Eigenmetabolite: A single value summarizing the information contained in the first principal component of PCA, which can, therefore, be used as a signature of the metabolomic profile for determining differences between patients' groups.

Area under the receiver-operating-characteristic curve (AUC): Estimates the value of a given metabolite to discriminate patients with different traits (e.g., patients with ACLF versus those with AD).

Hierarchical clustering: A computational method that groups metabolites (or samples) into small clusters and then groups these clusters into increasingly higher level clusters. As a result, a dendrogram (i.e., tree) of connectivity emerges.

Unsupervised analysis: An analysis of the results of metabolite profiling that does not take external factors such as survival or clinical signs into account.

Supervised analysis: An analysis of the results of metabolite profiling that takes external factors into account.

Table 2. Characteristics of the study patients with acutely decompensated cirrhosis.*

Characteristic	Acute Decompensation (N=650)	ACLF (N=181)	<i>p</i> value	ACLF-1 (N=97)	ACLF-2 (N=65)	ACLF-3 (N=19)	<i>p</i> value
Demographical and clinical data							
Age, y, mean \pm SD	57.7 \pm 12.1	57.0 \pm 11.3	0.49	58.9 \pm 11.5	55.5 \pm 10.9	52.6 \pm 9.9	0.04
Male sex, n (%)	421 (64.8)	118 (65.2)	0.92	66 (68.0)	43 (66.2)	9 (47.4)	0.22
Ascites, n (%)	394 (60.9)	132 (73.3)	<0.01	66 (68.0)	51 (79.7)	15 (78.9)	0.22
Potential precipitating events of ACLF, n (%)							
Bacterial Infection	138 (21.3)	62 (34.6)	<0.01	28 (29.8)	22 (34.4)	12 (63.2)	0.02
Active alcoholism	74 (11.4)	32 (17.7)	0.08	11 (11.6)	16 (24.6)	5 (26.3)	0.10
Other precipitating event	14 (2.2)	13 (7.2)	<0.01	5 (5.2)	7 (10.8)	1 (5.3)	0.38
No precipitating event	309 (50.1)	76 (43.9)	0.15	50 (53.2)	22 (36.7)	4 (21.1)	0.01
Organ system failures, n (%)							
Liver	44 (6.8)	71 (39.2)	<0.01	21 (21.7)	36 (55.4)	14 (73.7)	<0.01
Kidney	0 (0)	105 (58.0)	<0.01	63 (65.0)	27 (41.5)	15 (79.0)	<0.01
Brain	16 (2.5)	35 (19.3)	<0.01	3 (3.1)	21 (32.3)	11 (57.9)	<0.01
Coagulation	16 (2.5)	44 (24.3)	<0.01	6 (6.2)	26 (40.0)	12 (63.2)	<0.01

Table 2. (Continued)

Circulation	4 (0.6)	29 (16.0)	<0.01	1 (1.0)	14 (21.5)	14 (73.7)	<0.01
Respiration	3 (0.5)	14 (7.7)	<0.01	3 (3.1)	6 (9.2)	5 (26.3)	<0.01
Organ dysfunctions, n (%)							
Liver	99 (15.2)	25 (13.8)	0.64	14 (14.4)	10 (15.4)	1 (5.3)	0.51
Kidney	64 (9.9)	20 (11.1)	0.63	11 (11.3)	6 (9.2)	3 (15.8)	0.72
Brain	153 (23.5)	74 (40.9)	<0.01	50 (51.6)	17 (26.2)	7 (36.8)	<0.01
Number of deaths (%)							
By 28 days	31 (4.8)	48 (26.5)	<0.01	17 (17.5)	18 (27.7)	13 (68.4)	<0.01
By 90 days	81 (12.5)	73 (40.3)	<0.01	30 (30.9)	30 (46.2)	13 (68.4)	<0.01
Physiological variables							
Serum bilirubin, mg/dL, mean \pm SD	4.6 \pm 5.3	11.2 \pm 11.4	<0.01	6.7 \pm 8.0	14.2 \pm 10.7	24.4 \pm 14.9	<0.01
International normalized ratio, mean \pm SD	1.5 \pm 0.4	2.0 \pm 0.9	<0.01	1.6 \pm 0.5	2.4 \pm 0.9	2.9 \pm 1.2	<0.01
Median values of aminotransferases (IQR), U/L							
Alanine aminotransferase	34.5 (22-55)	35 (22-55)	0.99	29.5 (17.5-46.5)	37.5 (28-54)	58 (31-129)	<0.01
Aspartate aminotransferase	61.5 (38-99)	66 (37-111)	0.41	49.5 (33-91)	76 (46-111)	122.5 (88.5-149)	<0.01
Hematocrit, %, mean \pm SD	31.1 \pm 5.8	29.2 \pm 5.9	<0.01	29.5 \pm 5.8	29.3 \pm 5.1	26.9 \pm 8.6	0.25

Table 2. (Continued)

Serum creatinine, mg/dL, mean \pm SD	1.0 \pm 0.4	2.4 \pm 1.5	<0.01	2.5 \pm 1.5	1.9 \pm 1.5	2.9 \pm 1.9	<0.01
Blood white-cell count, $\times 10^9/L$, mean \pm SD	6.7 \pm 4.1	9.9 \pm 7.1	<0.01	8.1 \pm 4.7	11.2 \pm 7.0	14.6 \pm 13.2	<0.01
Median levels of blood glucose (IQR), mg/dL	107 (89-138)	109 (88-144)	0.85	108 (89-155)	107.7 (86-133.5)	116.5 (84.5-153)	0.52
Median values for inflammatory cytokines (IQR), pg/mL							
Tumor necrosis factor	20.4 (14.6-29.3)	29.4 (17.3-42.8)	<0.01	30.3 (20.3-44.7)	26.1 (16.4-36.5)	31.8 (17.2-42.7)	0.24
Interleukin-6	21.1 (9.8-44.5)	39.7 (15.0-117.8)	<0.01	32.3 (13.8-91.6)	43.5 (12.8-120.1)	97.9 (32.2-450.5)	0.03
Interleukin-8	41.6 (22.2-83.9)	89.3 (40.6-176.8)	<0.01	60.6 (35.6-121.8)	110.0 (67.8-192.1)	191.3 (111.8-371.8)	<0.01
Macrophage inflammatory protein 1-beta	23.2 (13.8-37.5)	26.5 (17.9-45.3)	0.02	24 (16.2-37)	29.7 (19.1-54.9)	45.3 (19.7-60.5)	0.08
Granulocyte-colony stimulating factor	21.5 (11.2-50.9)	29.9 (13.2-81.6)	0.02	30.5 (13.9-74.3)	29.1 (11.7-81.6)	43.3 (15.2-208.7)	0.59
Interleukin-10	3.4 (0.9-9.9)	6.8 (1.6-25.6)	<0.01	3 (0.9-11.4)	13.2 (3.2-43.7)	12.9 (10.8-55.0)	<0.01
Interleukin-1 receptor antagonist	11.4 (5.1-26.5)	21.6 (8.6-63.4)	<0.01	15.7 (8.0-36.9)	27.9 (8.7-67.9)	88.3 (23.8-189.8)	0.01
Median values for markers of leukocyte activation (IQR), mg/L							
Soluble CD163	8.0 (4.8-11.9)	13.8 (7.9-19.0)	<0.01	9.6 (5.9-18.1)	15.6 (10.1-19.7)	20.2 (16.3-32.2)	<0.01
Soluble macrophage mannose receptor 1	0.8 (0.5-1.1)	1.0 (0.7-1.5)	<0.01	0.8 (0.6-1.3)	1.1 (0.9-1.6)	1.4 (1.1-1.8)	<0.01

*Patients whose characteristics are shown here were enrolled in the CANONIC study (ref. 1). ACLF denotes acute-on chronic liver failure.

Table 3. Metabolites whose increased blood levels may affect the clinical phenotypes or indicate their bacterial origin in patients with ACLF.

Metabolite	Description	Potential Bacterial Origin
Related to glucose-6-phosphate		
Pentose phosphates	Molecules of the pentose phosphate pathway (PPP, which is branch of glycolysis) (see Fig. S1B)	
Pentose alcohols	Can give rise to molecules of the PPP	
D-Threitol	Related to PPP	
D-Glucuronic acid	Involved in glucuronidation which uses UDP-glucuronic acid (glucuronic acid linked via a glycosidic bond to uridine diphosphate) as an intermediate; UDP-glucuronic acid is formed in the liver; can give rise to metabolites of PPP	
Related to other carbohydrates		
D-Galacturonic acid	Is a sugar acid, the oxidized form of D-galactose	Yes
Trisaccharides	Can be either Maltotriose or D-Raffinose	
Related to the non-essential amino acid alanine		
N-Acetyl-L-alanine		Yes
Related to the non-essential amino acid aspartate		
N-Acetyl-aspartyl-glutamate (NAAG)	Metabolite of aspartate; localized to subpopulations of glutamatergic, cholinergic, GABAergic, and noradrenergic neuronal systems;	

released upon depolarization by a Ca^{2+} -dependent process; agonist at mGluR3 receptors and an antagonist at N-Methyl-D-aspartate (NMDA) receptors

N-Acetyl-L-aspartic acid

Metabolite of aspartate; precursor of NAAG; osmolyte; neurotoxic; high blood levels can cause metabolic acidosis

**Related to the essential amino acid
tryptophan†**

L-Kynurenine

Tryptophan metabolite; can act as an endothelium-derived relaxing factor; is neuroactive; has immunomodulatory effects

Kynurenic acid

Tryptophan metabolite; neuronal NMDA receptor antagonist; has immunomodulatory effects

Quinolinic acid

Tryptophan metabolite; first fully committed precursor in the *de novo* biosynthesis of NAD^+ ; agonist of neuronal NMDA receptor; may contribute to the generation of reactive oxygen species and nitric oxide

Indolelactic acid

Tryptophan metabolite produced by a pathway different from the kynurenine pathway

**Related to the essential amino acid
phenylalanine†**

N-Acetyl-L-phenylalanine

Metabolite of phenylalanine; accumulates in phenylketonuria which is a human genetic disorder due to the lack of phenylalanine

	hydroxylase, the enzyme necessary to metabolize phenylalanine to tyrosine	
Phenyllactic acid	Product of phenylalanine catabolism; accumulates in phenylketonuria	Yes
Hydroxyphenylacetic acids	Metabolites of phenylalanine and tyrosine; can give rise to pyruvate, acetoacetate, Krebs' cycle intermediates (succinate, fumarate)	
Related to the essential amino acid methionine		
Cystathionine	Metabolite of methionine (the transsulfuration of methionine yields homocysteine, which combines with serine to form cystathionine, through the enzymatic activity of cystathionase); proximal precursor of cysteine (cysteine can give rise to pyruvate and hydrogen sulfide [H ₂ S])	
5'-Deoxy-5'-(Methylthio)adenosine (also known as MTA)	Methionine metabolite, produced from S-adenosylmethionine through the polyamine biosynthetic pathway; can be metabolized by MTA-phosphorylase, to yield 5-methylthioribose-1-phosphate and adenine, a crucial step in the methionine and purine salvage pathways, respectively	
N-Formyl-L-methionine	Metabolite of methionine; involved in the initiation of translation of mRNA into proteins	Yes

**Related to the essential amino acid arginine
and the non-essential proline**

4-Acetamidobutanoic acid

Gamma-aminobutyric acid (GABA) derivative; product of the urea cycle and the metabolism of amino groups; product of NAD-linked aldehyde dehydrogenase

Related to the essential amino acid lysine†

L-Saccharopine

Intermediate of lysine degradation; can give rise to pipercolate, acetyl-Coenzyme A (CoA), acetoacetate; high blood levels can cause metabolic acidosis

N6,N6,N6-Trimethyl-L-lysine

Is generated by the action of S-adenosyl-L-methionine on exposed lysine residues found in a number of proteins; is released from cognate proteins via proteolysis to serve as a precursor for carnitine biosynthesis

Fatty acyl carnitines

Hexanoylcarnitine

Composed of a fatty acid attached to carnitine; accumulates in blood in patients with medium-chain acyl-CoA dehydrogenase deficiency

Octanoylcarnitine

Composed of a fatty acid attached to carnitine; accumulates in blood in patients with medium-chain acyl-CoA dehydrogenase deficiency

Related to succinate

May contribute to anaplerotic reactions (replenishment of intermediates of the Krebs' cycle)

Related to the essential amino acid tyrosine†

Phenol

Immunomodulatory effects; antioxidant

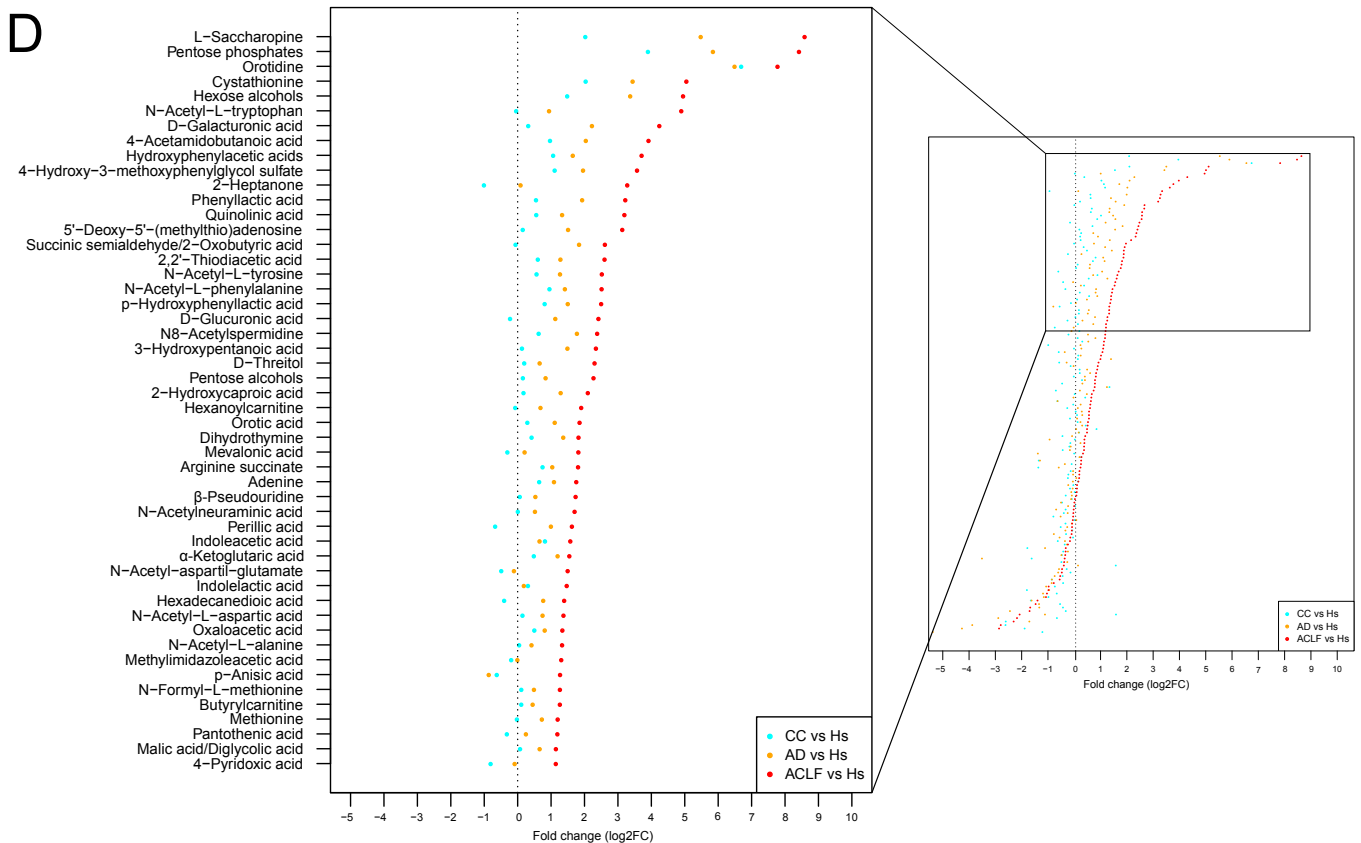
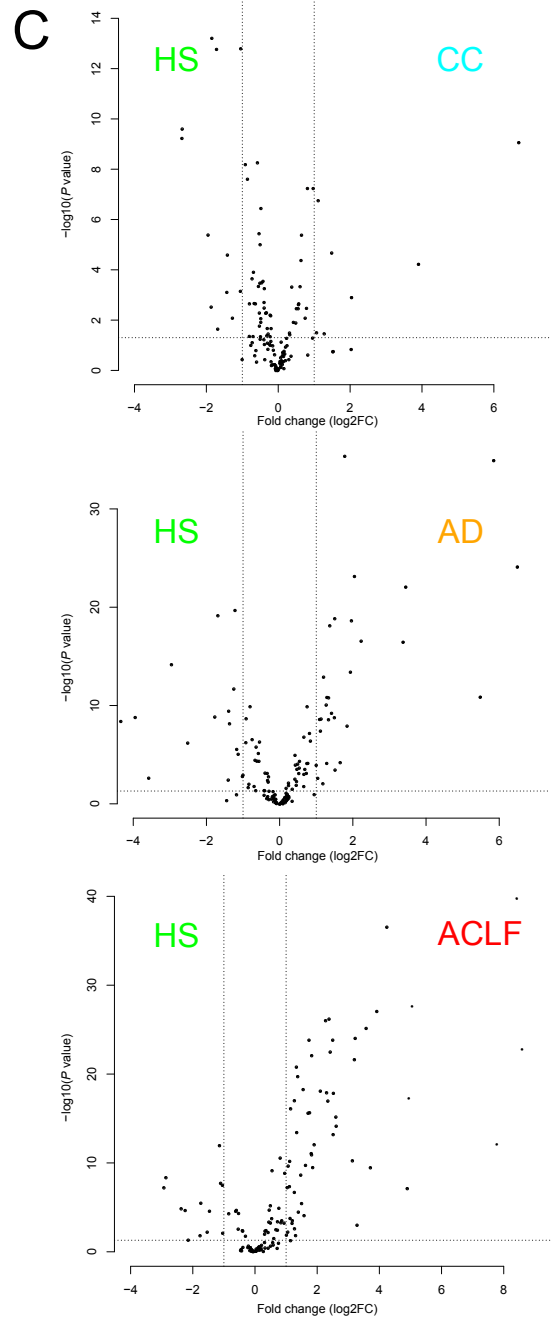
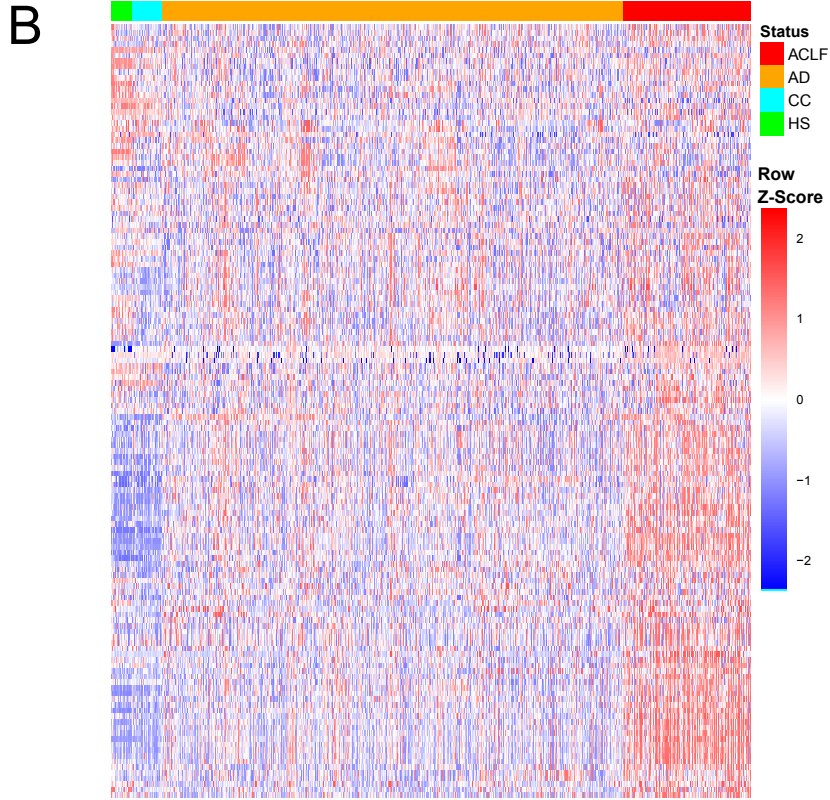
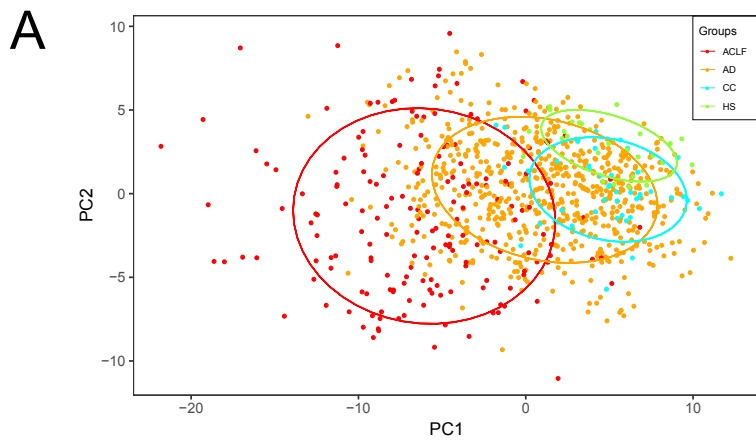
Yes

N-Acetyl-L-tyrosine	Converts to tyrosine	
p-Hydroxyphenyllactic acid	Tyrosine metabolite; accumulates in phenylketonuria and tyrosinemia	Yes
p-Anisic acid	Phenolic acid; non-competitive inhibitor of the hydroxylation of L-tyrosine catalyzed by tyrosinase, and oxidation of L-3,4-dihydroxyphenylalanine (L-DOPA)	Yes
Other metabolites		
β-Pseudouridine	C-glycoside isomer of the nucleoside uridine; involved in translation of mRNA into proteins; the most prevalent of the over one hundred different modified nucleosides found in RNA; enhances the function of transfer RNA and ribosomal RNA by stabilizing the RNA structure.	
4-Hydroxy-3-methoxyphenylglycol sulfate	Sulfated metabolite of brain norepinephrine; possible marker of central norepinephrine turnover	
N-Acetylneuraminic acid (sialic acid)	Binds to glycans; recognition of sialic acid-containing glycans by SIGLEC10 helps the immune system to distinguish “self” and “non-self”; recognition of sialic acid-containing glycans on CD24 inhibits TLR inflammatory signaling; can be released from these glycans by the action of bacterial sialidases	
Mevalonic acid	Precursor in the HMG-CoA reductase pathway, that produces terpenes and steroids	
2-Heptanone	Belongs to the class of organic compounds known as ketones	Yes
2,2'-Thiodiacetic acid	May be a product of xenobiotic metabolism by cytochrome P450	

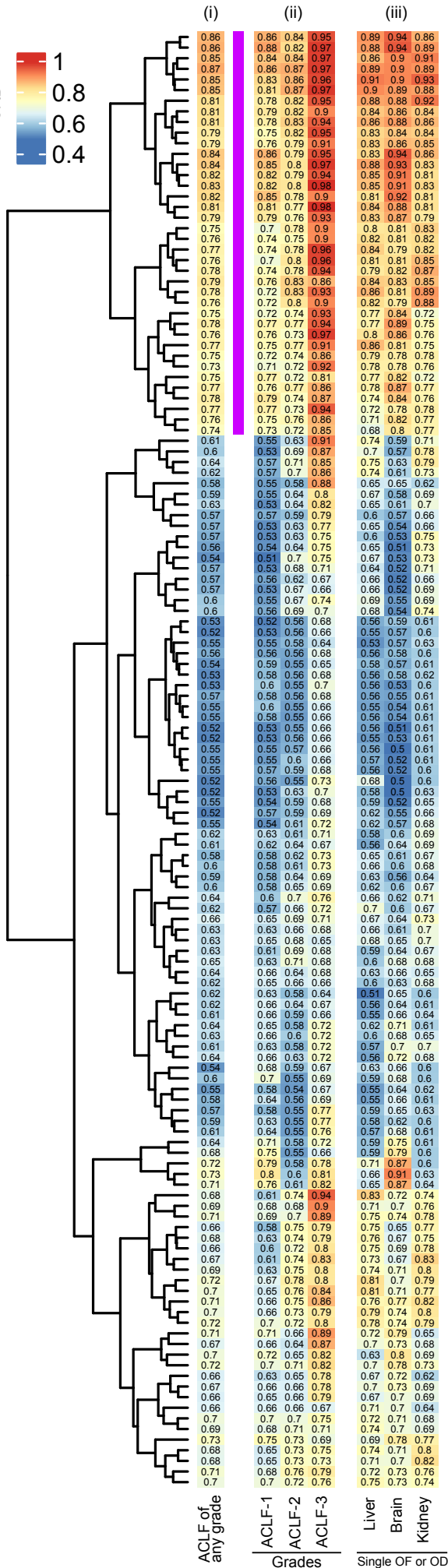
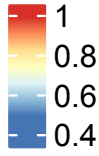
Pantothenic acid (also known as vitamin B5)	Needed to form coenzyme-A (CoA).	
N-Acetyl-L-tryptophan	Metabolic pathway uncertain; substance P receptor blocker	
L-(+)-Tartaric acid	Can give rise to Krebs' intermediate oxaloacetate	Yes

* Metabolites are listed according to the color code used in Figure 2B. NADP denotes nicotinamide adenine dinucleotide phosphate, UDP uridine diphosphate, mGluR3 metabotropic glutamate receptor 3, NAD⁺ nicotinamide adenine dinucleotide, SIGLEC sialic acid-binding Ig-like lectin, TLR Toll-like receptor, and HMG-CoA (S)-3-Hydroxy-3-methylglutaryl-CoA.

† Amino acid known to be involved in ketogenesis.



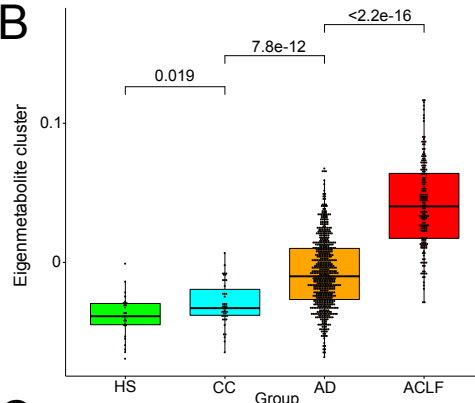
A

AUC ACLF
vs AD

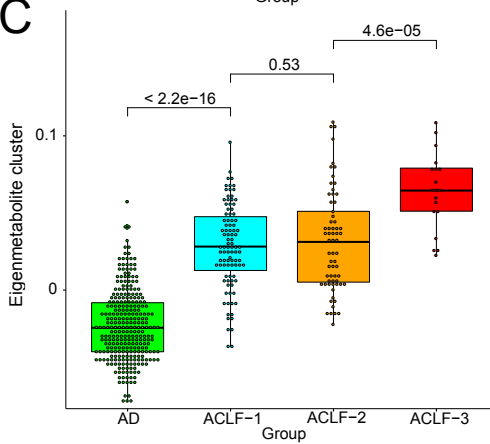
ACLF Associated Metabolite Cluster

β-Pseudouridine
 Pentose alcohols
 Pentose phosphates
 N-Acetyl-L-alanine
 D-Galacturonic acid
 N-Acetyl-aspartil-glutamate
 D-Glucuronic acid
 L-Kynurenine
 4-Hydroxy-3-methoxyphenylglycol sulfate
 N-Acetyl-L-phenylalanine
 Cystathionine
 D-Threitol
 4-Acetamidobutanoic acid
 N-Acetylneuraminic acid
 Quinolinic acid
 Mevalonic acid
 L-Saccharopine
 Hydroxyphenylacetic acids
 Phenyllactic acid
 N-Acetyl-L-aspartic acid
 Hexanoylcarnitine
 p-Hydroxyphenyllactic acid
 5'-Deoxy-5'-(methylthio)adenosine
 N-Formyl-L-methionine
 N-Acetyl-L-tyrosine
 Related to Succinate
 2-Heptanone
 Kynurenic acid
 N6,N6,N6-Trimethyl-L-lysine
 Trisaccharides
 2,2'-Thiodiacetic acid
 Octanoylcarnitine
 Pantothenic acid
 Indolelactic acid
 p-Anisic acid
 Phenol
 N-Acetyl-L-tryptophan
 L-(+)-Tartaric acid

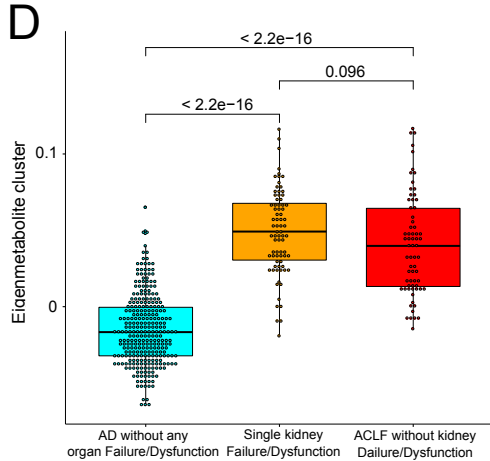
B



C

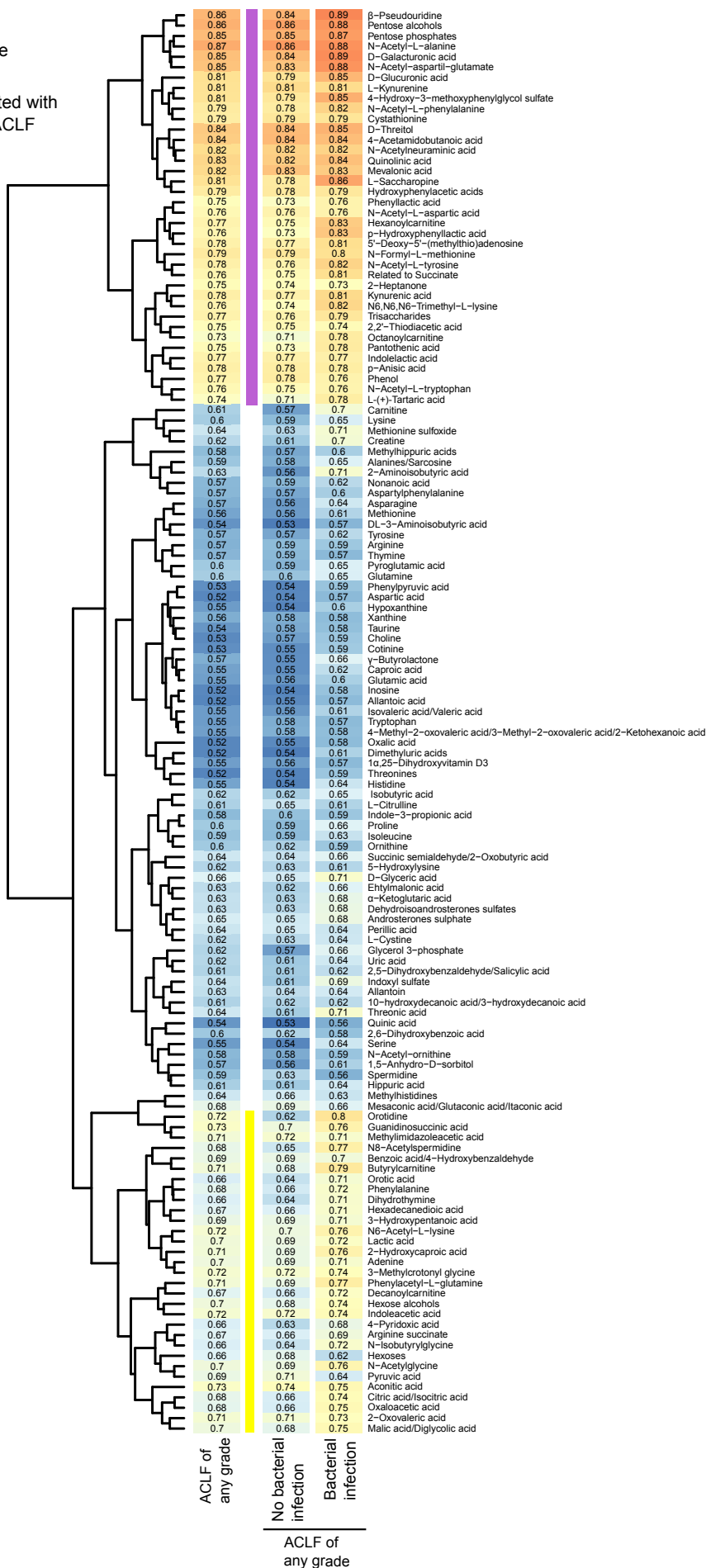
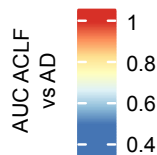


D

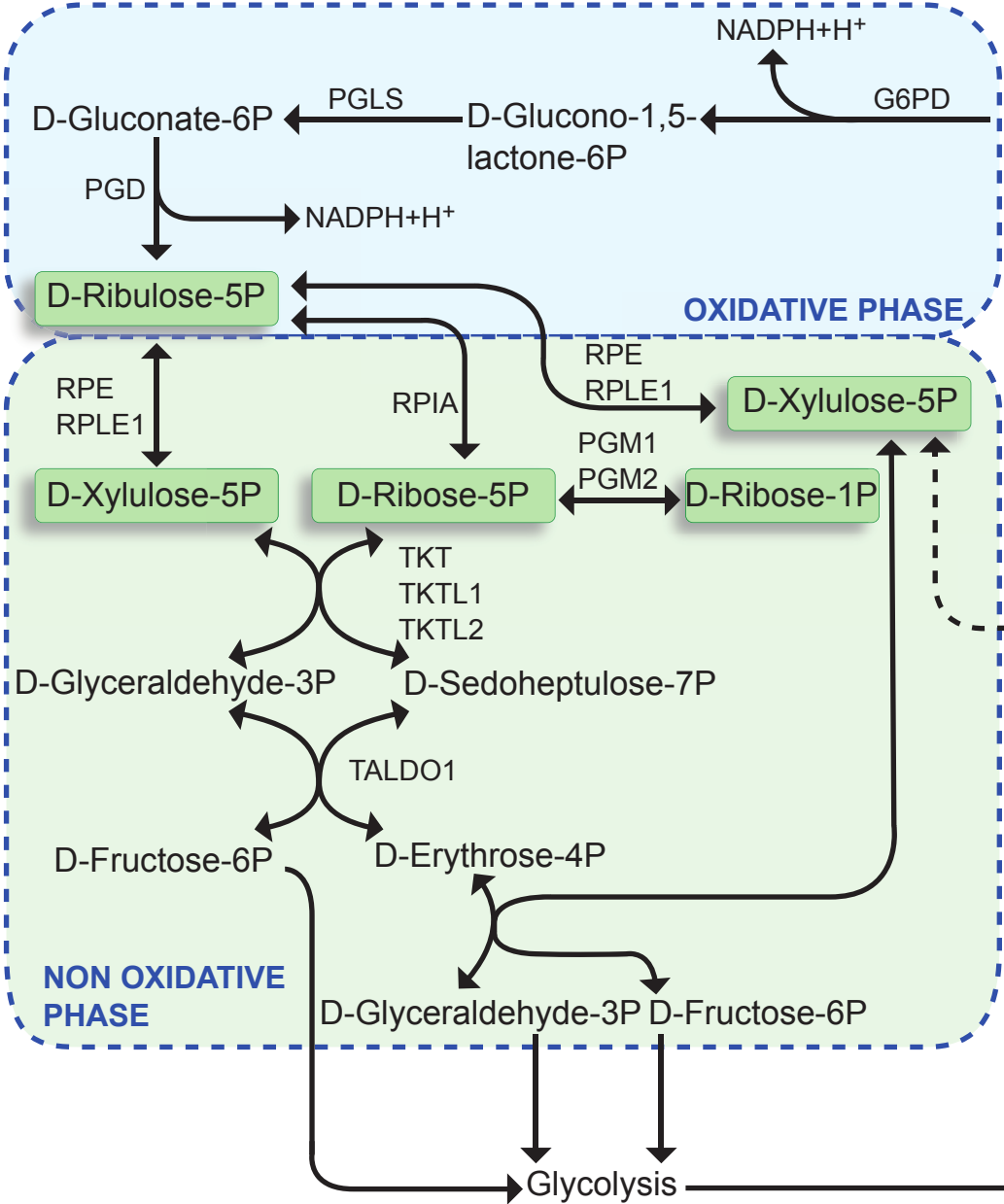


ACLF metabolite
fingerprint

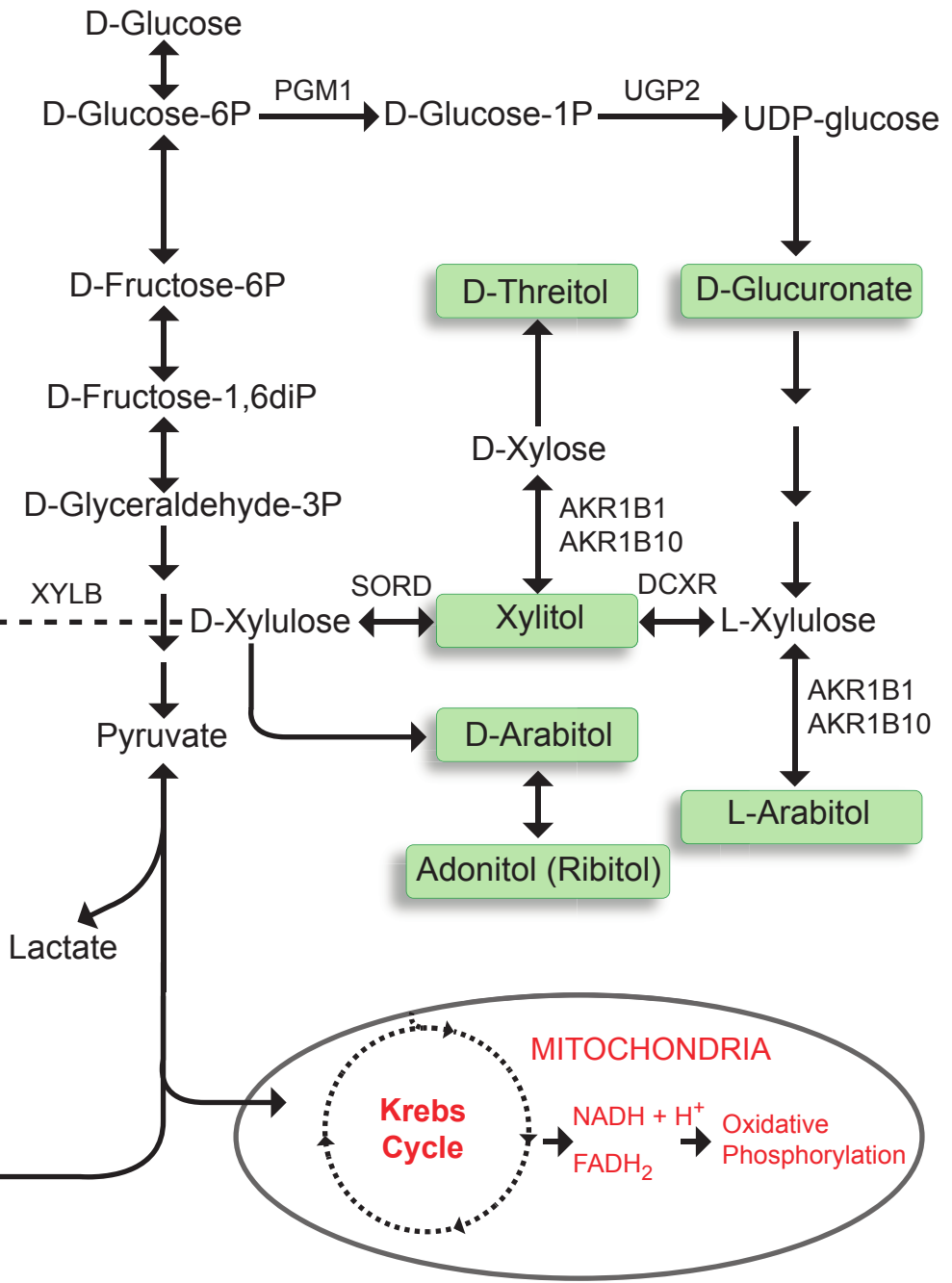
Cluster associated with
sepsis-related ACLF



PENTOSE PHOSPHATE PATHWAY



GLUCURONATE PATHWAY

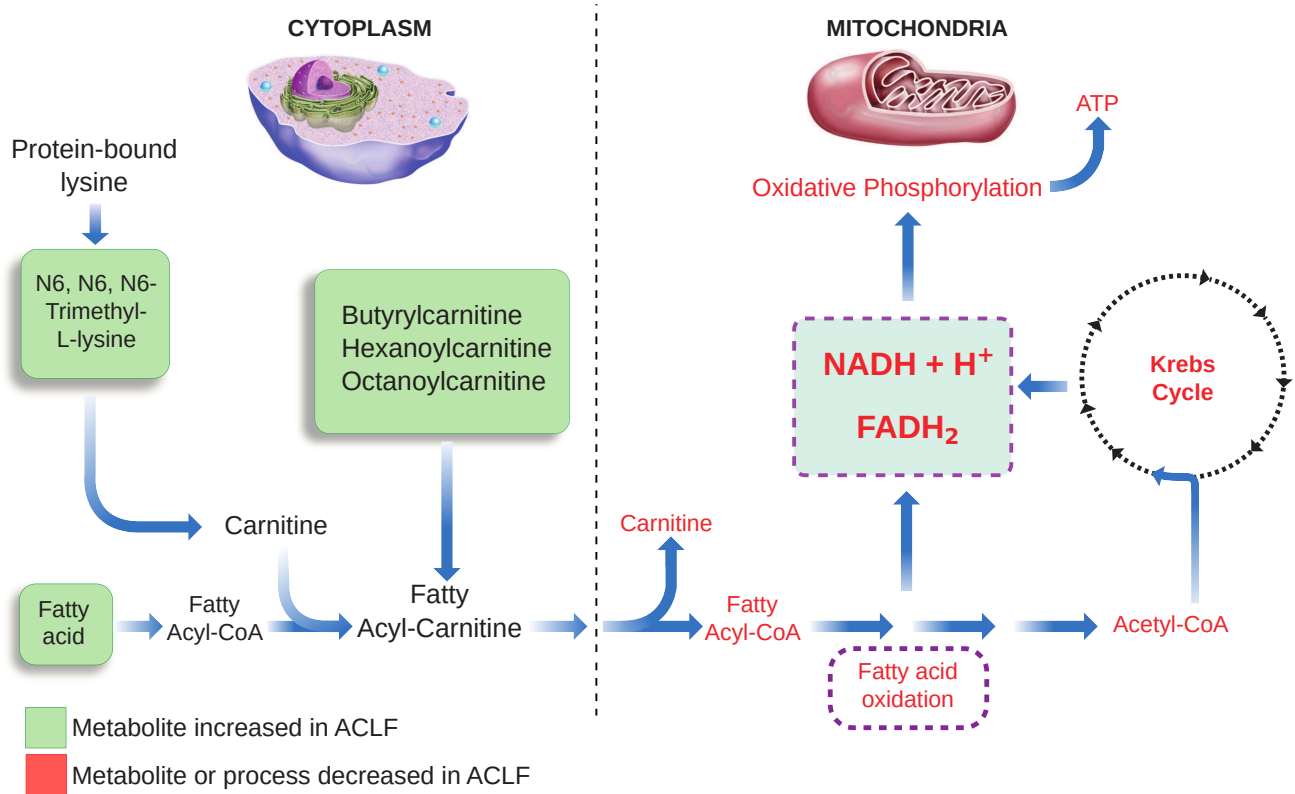


Metabolites increased in ACLF

Metabolites or processes decreased in ACLF

A

Name of the Acylcarnitine	Length of the fatty acid attached to Carnitine	Fold Change values (ACLF vs HS)
Butyrylcarnitine	Short-chain	2.43
Hexanoylcarnitine	Medium-chain	3.79
Octanoylcarnitine	Medium-chain	1.80

B

Graphical Abstract

Persons involved in the study



n=181
Patients with ACLF

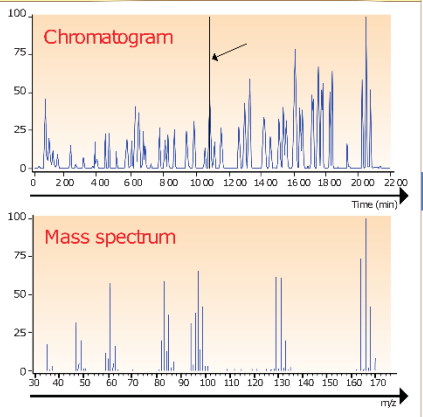
n=650
Patients with AD

n=43
Patients with compensated cirrhosis

n=29
Healthy subjects

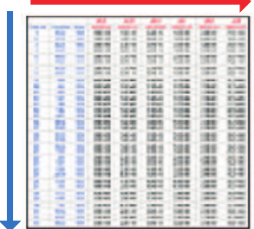
Biobanked serum samples

Metabolome analysis



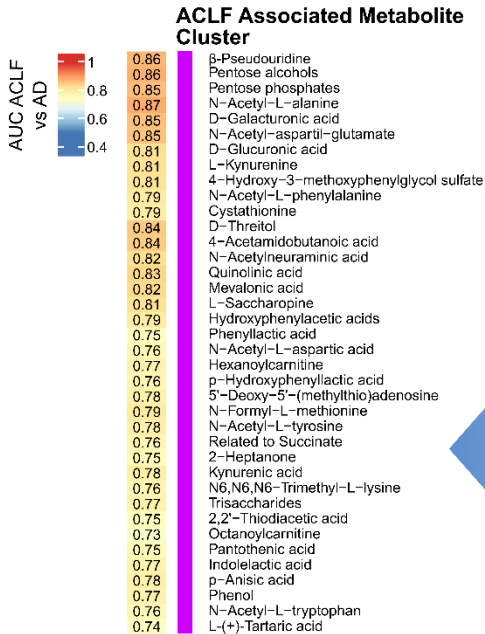
Data processing

Automatic detection of signals



Selection of relevant features

Annotation databases public/internal



AUC of metabolites for ACLF vs AD
Hierarchical cluster analysis of AUCs
Eigenmetabolites computation

Identification of a blood metabolome fingerprint specific for ACLF

PCA
Unsupervised hierarchical cluster analysis of blood metabolites
Between-group pairwise comparisons

Identification of blood metabolome changes across study groups